Molecular Biology of the Cell
Vol. 20, 2650–2660, June 1, 2009

Reactive Oxygen Species Regulate a Slingshot-Cofilin Activation Pathway

Jun-Sub Kim, Timothy Y. Huang, and Gary M. Bokoch

Department of Immunology and Microbial Science and Department of Cell Biology, The Scripps Research Institute, La Jolla, CA 92037

Submitted February 13, 2009; Revised March 20, 2009; Accepted March 24, 2009
Monitoring Editor: Jonathan Chernoff

Cellular stimuli generate reactive oxygen species (ROS) via the local action of NADPH oxidases (Nox) to modulate cytoskeletal organization and cell migration through unknown mechanisms. Cofilin is a major regulator of cellular actin dynamics whose activity is controlled by phosphorylation/dephosphorylation at Ser3. Here we show that Slingshot-1L (SSH-1L), a selective cofilin regulatory phosphatase, is involved in H_2O_2-induced cofilin dephosphorylation and activation. SSH-1L is activated by its release from a regulatory complex with 14-3-3ζ protein through the redox-mediated oxidation of 14-3-3ζ by H_2O_2. The ROS-dependent activation of the SSH-1L-cofilin pathway stimulates the SSH-1L–dependent formation of cofilin-actin rods in cofilin-GFP–expressing HeLa cells. Similarly, the formation of endogenous ROS stimulated by angiotensin II (AngII) also activates the SSH-1L-cofilin pathway via oxidation of 14-3-3ζ to increase AngII-induced membrane ruffling and cell motility. These results suggest that the formation of ROS by NADPH oxidases engages a SSH-1L-cofilin pathway to regulate cytoskeletal organization and cell migration.

INTRODUCTION

Cell migration is required for many normal biological processes, including embryonic morphogenesis, immune surveillance, and tissue repair and regeneration. Aberrant regulation of cell migration can also drive disease progression, including cancer invasion and metastasis (Yamaguchi and Condeelis, 2007). Cell migration requires the activation of the underlying motility cycle, the first step of which is cell protrusion driven by actin polymerization (Ridley *et al.*, 2003). The extension of protrusions initiates cell movement and defines the direction of migration (Condeelis, 1993). The early steps in actin polymerization are controlled by Arp2/3-mediated actin nucleation and branching, as well as formin-mediated actin filament extension (Higgs and Pollard, 2001; Pruyne *et al.*, 2002). These act along with cofilin-dependent actin severing and depolymerization, which provides actin monomers for further polymerization, to drive actin treadmilling and membrane protrusion (Svitkina and Borisy, 1999). There is substantial evidence that the expression of genes regulating cofilin activity are altered in invasive tumor cells (Wang *et al.*, 2007).

Cofilin activity can be regulated through a variety of upstream effectors reviewed in (Bamburg, 1999). One of the primary mechanisms for controlling cofilin activity is through the regulation of its phosphorylation at the Ser3 regulatory site, which phosphocycles between phosphorylated (inactive) and nonphosphorylated (active) states. The LIM kinases 1 and 2 phosphorylate cofilin on Ser3, rendering it unable to bind to F-actin and thus inactive (Arber *et al.*, 1998; Yang *et al.*, 1998). The protein phosphatase Slingshot (SSH) and the novel HAD-family phosphatase, chronophin (CIN), are the primary dedicated cofilin phosphatases that dephosphorylate cofilin at Ser3 and activate it in a variety of cell types (Niwa *et al.*, 2002; Gohla *et al.*, 2005; Huang *et al.*, 2006). SSH activity can be modulated through several mechanisms, including F-actin binding (Niwa *et al.*, 2002), calcium acting via calcineurin (Wang *et al.*, 2005), and by its association in inhibitory complexes with 14-3-3 regulatory proteins (Nagata-Ohashi *et al.*, 2004; Soosairajah *et al.*, 2005).

Reactive oxygen species (ROS) function as signaling molecules to mediate various biological responses, including cell growth and gene expression, host defense, and even cell migration (Bedard and Krause, 2007). ROS are short-lived, diffusible molecules. Therefore, the localization of the ROS signal at specific subcellular compartments may be essential for initiating redox-dependent, spatially restricted signaling events after receptor activation (Ushio-Fukai, 2008). NADPH oxidases (Nox) are one of the major regulatable enzymatic sources of ROS in various tissues (Bedard and Krause, 2007). Nox consist of a catalytic subunit (Nox1, Nox2, Nox3, Nox4, and Nox5 and Duox 1 or 2) whose activity is controlled by various combinations of regulatory subunits, including a membrane localized cosubunit (p22phox), various organizer (e.g., p47phox, NoxO1), and activator (e.g., p67phox, NoxA1) subunits, and the small guanosine triphosphatase Rac1 (or Rac2 in leukocytes; Bokoch and Knaus, 2003; Bedard and Krause, 2007; Lambeth *et al.*, 2007).

The renin–angiotensin system has been implicated in both angiogenesis and pathological vascular growth (Mehta and Griendling, 2007). In vitro, stimulation of the angiotensin II type 1 receptor (AT1R) induces migration of vascular smooth muscle cells and promotes endothelial cell proliferation (Lassegue and Clempus, 2003; Mehta and Griendling, 2007). Recent studies have revealed localized expression of components of the renin–angiotensin system in various cancer cells and tissues (Deshayes and Nahmias, 2005). Angiotensin II (AngII) is a potent stimulator for vascular and renal NADPH oxidases (Garrido and Griendling, 2008), particu-

This article was published online ahead of print in *MBC in Press* (http://www.molbiolcell.org/cgi/doi/10.1091/mbc.E09–02–0131) on April 1, 2009.

Address correspondence to: Gary M. Bokoch (bokoch@scripps.edu).

larly Nox1 (Lassegue *et al.*, 2001). Although Nox1 is abundant in colon epithelial cells, it is also found in many other tissues that respond to AngII stimulation (Garrido and Griendling, 2008). Nox1 activity requires p22phox along with the organizer subunit NoxO1, the activator subunit NoxA1, and Rac1 GTPase (Bokoch and Knaus, 2003; Bedard and Krause, 2007; Lambeth *et al.*, 2007). AngII has been shown to stimulate Rac1 activity to regulate ROS production via Nox1 (Lassegue *et al.*, 2001; Garrido and Griendling, 2008).

Nox-mediated ROS formation is required for motility in a variety of cell types (e.g., endothelial and epithelial cells, vascular smooth muscle cells, neurons, and fibroblasts; Moldovan *et al.*, 2000; Weber *et al.*, 2004; Ikeda *et al.*, 2005; Schroder *et al.*, 2007; Munnamalai and Suter, 2008; Sadok *et al.*, 2008). It is of note that cancer cell metastasis has long been linked to the formation of ROS (Szatrowski and Nathan, 1991; Nonaka *et al.*, 1993; Soares *et al.*, 1994; Wu, 2006). Recently, ROS-generating mitochondrial mutations have been shown to regulate tumor cell metastasis (Ishikawa *et al.*, 2008). Nox1 is overexpressed in colon cancers, and its activity is strongly correlated with the presence of oncogenic K-Ras mutations (Laurent *et al.*, 2008). However, the mechanisms by with ROS contribute to cell migration have not been well defined at the molecular level. ROS have been shown to regulate growth factor signaling in general through their inhibitory effects on protein tyrosine phosphatases (Tonks, 2005). More specific interactions that may affect cell migration include ROS-induced p38 MAP kinase activation (Djordjevic *et al.*, 2005), JNK-dependent phosphorylation of the focal adhesion protein, paxillin (Schroder *et al.*, 2007), and interactions of Nox with cytoskeletal regulators such as IQGAP (Ikeda *et al.*, 2005) and WAVE (Wu *et al.*, 2003). In a separate study, platelet-derived growth factor (PDGF)-induced vascular smooth muscle cell migration was ROS-dependent and required activity of both Src and the Rac effector, PAK1 (Weber *et al.*, 2004). Subsequent work established that ROS induced the dephosphorylation of cofilin in smooth muscle cells, associated with an increase in barbed end actin incorporation (San Martin *et al.*, 2008). A transient activation of LIMK1 by PDGF was accompanied by a more persistent activation of the cofilin phosphatase SSH. The mechanism by which ROS regulated SSH activity in this study was not determined.

In the current article, we examine the cellular mechanism by which ROS regulates cofilin dephosphorylation and cytoskeletal rearrangements in HeLa cells. Our data define a direct role of ROS in the regulation of the SSH cofilin phosphatase to modulate cofilin activity and cell migration induced by AngII.

MATERIALS AND METHODS

Cell Culture and Transfection

HeLa cells, eGFP-cofilin1–expressing stable HeLa cells (Huang *et al.*, 2008), and MCF-7 cells were maintained in DMEM (Invitrogen, Carlsbad, CA) containing 10% heat-inactivated fetal bovine serum (Invitrogen), 1 mM sodium pyruvate, 100 μM nonessential amino acids, and antibiotics (100 U/ml penicillin and 100 μg/ml streptomycin) at 37°C in 5% CO_2. The cells were transfected with vectors harboring the inserted gene or siRNA, using Lipofectamine 2000 according to the manufacturer's instructions.

Plasmid, Small Interfering RNA, and Short Hairpin RNA Construction

pRK5-myc-Nox1, -NoxO1, -NoxA1, -Rac1-CA, pcDNA3.1-HA-14-3-3ζ-wt and -K49E, and pcDNA3-HA-AT1R were described previously (Kim *et al.*, 2007). pcDNA3-SSH-1L-GST, pcDNA3-cofilin-HA-his6, si-Control, -SSH-1L, and -CIN RNA vectors were described previously (Huang *et al.*, 2008). pcDNA3 mRFP/H1-SSH-1L was constructed by inserting a SSH-1L–targeting short hairpin RNA (shRNA) sequence corresponding to TCGTCACCCAAGAAAGATA (Wang *et al.*, 2005) downstream of an H1 promoter sequence.

Western Blot

Six-well cultured HeLa or MCF-7 cells were serum-starved for 16 h and then treated with 0.5 mM H_2O_2 or 0.1 μg/ml AngII (Bachem, Torrance, CA) for 0–30 min at 37°C after pretreatment with inhibitors for 0.5 h (0.1 mM Na_3VO_4, 10 μM LY294002 [LY], 100 nM wortmannin [Wort], 1 μM okadaic acid [OA], 1 μM calyculin A [CalA], 30 μM BAPTA-AM, 1 mM EGTA, or 10 μM diphenyliodonium [DPI], all from Sigma, St. Louis, MO). The cells were lysed in RIPA buffer (25 mM Tris·HCl pH 7.6, 150 mM NaCl, 1% NP-40, 1% sodium deoxycholate, 0.1% SDS, 0.1 mM Na_3VO_4, 1 mM phenylmethylsulfonyl fluoride, and 1 μg/ml each aprotinin, leupeptin, and benzamidine). Thirty micrograms of cleared lysate protein was analyzed by SDS-PAGE and Western blotting. Phospho-cofilin levels were normalized for total cofilin by densitometric analysis. Antibodies for immunoblotting were as follows: anti-Myc (M4439; Sigma), anti-HA (1-867-423; Roche Diagnostics, Indianapolis, IN), anti-pan-14-3-3 and anti-pan-14-3-3ζ (SC629 and SC1019, respectively; Santa Cruz Biotechnology, Santa Cruz, CA), anti-SSH-1L (SP1711; ECM Biosciences, Versailles, KY), anti-actin (691002; MP Biomedicals, Solon, OH), anti-phospho-cofilin (3311; Cell Signaling, Beverly, MA), anti-cofilin (ACFL02A; Cytoskeleton, Denver, CO), and anti-phospho-LIMK1/2 (07-850; Millipore, Bedford, MA). Antibody to CIN has been described previously (Gohla *et al.*, 2005).

5′-Fluorescein Iodoacetamide Labeling

Labeling was performed by the slight modification of the method described previously (Wu *et al.*, 1998). Cells were lysed in lysis buffer (50 mM MES-NaOH, pH 7.5, 0.5% Triton X-100, 1 μg/ml leupeptin, 1 μg/ml aprotinin, and 1 mM PMSF) under anaerobic conditions. Lysates were clarified by a centrifugation at 100,000 $\times$ *g* for 15 min. The labeling reaction was performed by the addition of 10 μM iodoacetamide-fluorescein (Molecular Probes, Eugene, OR; cat. no. I30451) to lysates for 60 min at 4°C. The labeled lysates were immunoprecipitated with anti-Myc antibody for Myc-tagged proteins, anti-HA antibody for HA-14-3-3ζ or anti-14-3-3ζ antibody for endogenous 14-3-3ζ, and immunoprecipitates were analyzed by Western blotting with anti-FITC (Zymed, South San Francisco, CA; 71-1900).

Measurement of Reactive Oxygen Species

Reactive oxygen was measured using luminol chemiluminescence as described previously (Kim *et al.*, 2007). Transfected HeLa cells were cultured for 16 h and harvested by incubation with trypsin/EDTA for 1 min at 37°C. After washing with phosphate-buffered saline (PBS; without $MgCl_2$ and $CaCl_2$), the cells were removed from the well, washed twice with cold HBSS containing calcium and magnesium, then pelleted at 1000 $\times$ *g* for 5 min, and resuspended in HBSS. HeLa cells, 5×10^5, were used per assay and 2×10^5 MCF-7 cells per assay. Chemiluminescence was measured for 30 min with or without 100 ng/ml AngII at 37°C.

Protein Purification

p-Cofilin-HAhis6 was expressed in HeLa cells, lysed in phosphatase buffer with 10 mM imidazole and 1% NP40, precipitated with Ni-NTA agarose (Qiagen, Chatsworth, CA), and washed extensively in 25 mM imidazole. p-Cofilin-HAhis6 eluates were dialyzed in phosphatase buffer (20 mM HEPES, pH 7.5, 150 mM NaCl, 10 mM $MgCl_2$, and 5% glycerol) containing 1 mM DTT overnight at 4°C, and frozen at −80°C (Huang *et al.*, 2008).

In Vitro Phosphatase Assay

Cofilin dephosphorylation by glutathione *S*-transferase (GST) or GST-SSH-1L precipitates was measured in vitro using a p-cofilin-HAhis6 substrate purified from HeLa cells, as in Huang *et al.* (2008). Phosphorylated cofilin (p-Cofilin) dephosphorylation was determined by the disappearance of p-cofilin detected by immunoblotting using a phospho-specific antibody recognizing p-cofilin. Blots were stripped and reprobed with an anti-HA antibody to determine total cofilin in the assays, and p-cofilin levels were normalized for total cofilin by densitometric analysis.

In Vitro Pulldown Assay

In vitro pulldown assay was as previously described (Kim *et al.*, 2007). Lysates of HeLa cells expressing GST, GST-SSH-1L, and/or HA-14-3-3ζ were incubated with glutathione Sepharose. After centrifugation, the pellets were subjected to SDS-PAGE and analyzed by immunoblotting with an anti-GST or -HA antibody.

Cofilin Rod Formation

Enhanced green fluorescent protein (eGFP)-cofilin was visualized in cofilin-GFP–expressing HeLa cells seeded on glass coverslips by fixation in 4% paraformaldehyde at room temperature (RT) for 45 min, followed by extraction in cold methanol for 3 min, washing in PBS, and mounting on glass slides in anti-fade reagent (Prolong Gold, Molecular Probes), as described (Huang *et al.*, 2008). Before fixation, cofilin-GFP–expressing HeLa cells transfected with or without HA-14-3-3ζ-wt, -K49E, or shRNA vectors were preincubated with or without 0.1 mM vanadate for 30 min and then treated with or without

0.5 mM H_2O_2 for 30 min. Visualization of HA-14-3-3ζ was with anti-HA antibody and Alexa 350–conjugated goat anti-mouse IgG antibody (Molecular Probes). Fluorescence images were obtained with a 40× (see Figure 3A) or 20× (see Figure 5A) objective lens and processed by MetaMorph software (Universal Imaging, Downingtown, PA).

Cellular Localization of Cofilin and Nox1s

Cofilin-GFP-HeLa cells expressing the AT1R and the complete Nox1 system (Nox1s: Nox1, NoxA1, and NoxO1) were fixed on coverslips with 4% paraformaldehyde in PBS at 37°C for 30 min and then permeabilized with 0.5% Triton X-100 in PBS at RT for 5 min. The cells were washed with PBS and blocked by incubation with 5% bovine serum albumin (BSA)/PBS for 1 h. Coverslips were then incubated with antibody against Myc in PBS containing 2% BSA for 2 h at RT. After washing in PBS, the cells were incubated with Alexa 568–conjugated goat anti-mouse (Molecular Probes) or Alexa 568-phalloidin in 2% BSA/PBS for 1 h at RT and then washed with PBS and mounted for analysis. Fluorescence images were obtained with a 40× objective lens and processed by MetaMorph software.

Cell Migration Assay

For in vitro wound healing, a confluent layer of HeLa, MCF-7, small interfering RNA (siRNA)-treated HeLa or -MCF-7 cells were serum starved for 16 h and then scratched with a pipette tip. The culture medium was changed to remove detached cells or debris and then treated with or without AngII. phase-contrast images of the wound were taken at three random locations: first immediately after wounding and then at the same location after 24 h to examine wound closure by migrating cells. Cells that migrated into the delineated wound area were then counted using ImageJ software (http://rsb.info.nih.gov/ij/). MCF-7 cell in vitro Transwell (Millipore; Millicell 8 μm) migration assay was as described (Kim *et al.*, 2006). Type IV collagen was used to coat the membrane for 3 h and dried. Six hundred microliters serum-free DMEM with 0.1% BSA (wt/vol) and 0.1 μM AngII was added to the lower chamber, and cells in 200 μl serum-free DMEM were added to the upper chamber. Where indicated, 10 μM DPI was preincubated with cells for 30 min before loading in the upper chamber. After 24 h of migration, cells remaining on the upper membrane were scraped off, and cells that had migrated to the lower membrane were stained with 0.5% crystal violet/20% methanol. The crystal violet dye retained on the filters was resolved in 10% acetic acid and absorbance was colorimetrically measured at 595 nm.

Statistical Analysis

All statistical analyses presented were calculated using two-tailed Student's *t* test.

RESULTS

H_2O_2 Activates Cofilin through SSH Phosphatase

Several studies have shown that ROS formation induces the dephosphorylation (activation) of cofilin through unknown mechanisms. This includes neutrophils activated by the chemoattractant peptide fMLP (Heyworth *et al.*, 1997), and vascular smooth muscle cells stimulated with PDGF or treated with exogenous H_2O_2 (Lee *et al.*, 2006; San Martin *et al.*, 2008). To determine the molecular basis for cofilin dephosphorylation induced by ROS, we investigated whether one of the known cofilin phosphatases was required for H_2O_2-induced cofilin dephosphorylation. The Ser/Thr phosphatases PP1 and PP2A, the HAD-type phosphatase CIN, and SSH phosphatases have all been previously shown to dephosphorylate p-cofilin (Ambach *et al.*, 2000; Niwa *et al.*, 2002; Gohla *et al.*, 2005). In HeLa cells we observed that cofilin was totally dephosphorylated by exposure to H_2O_2 after 10 min and that this effect was not reversed over a 30-min period (Figure 1A). Steady-state p-cofilin levels were slightly increased in the presence of 1 μM okadaic acid or 1 μM calyculin A (Figure 1, A and B), each of which inhibits PP1 and PP2A (Cohen, 1990), as well as by 1 mM sodium vanadate, which is active toward a broad range of tyrosine- and dual-specificity-phosphatases, or BAPTA-AM and EGTA, both of which are calcium chelators and can inhibit PP2B and indirectly activate SSH-1L (Wang *et al.*, 2005). However, the dephosphorylation of p-cofilin upon H_2O_2 treatment was not blocked by any of the aforementioned inhibitors except vanadate (Figure 1B).

SSH-1L and CIN are known to be p-cofilin phosphatases that are insensitive to most phosphatase inhibitors other than vanadate (Niwa *et al.*, 2002; Gohla *et al.*, 2005). To establish whether one of these phosphatases is involved in vanadate-sensitive H_2O_2-mediated p-cofilin dephosphorylation, we depleted SSH-1L or CIN using siRNA (as previously described; Huang *et al.*, 2008; Figure 1C). Under basal conditions, knockdown of CIN, SSH-1L, or both in combination had no major effect on p-cofilin levels. Conversely, the knockdown of SSH-1L, but not CIN, led to a reversal of cofilin dephosphorylation induced by H_2O_2, and the accumulation of p-cofilin (Figure 1C). Knockdown of both SSH-1L and CIN increased the level of p-cofilin to a level comparable to that of SSH-1L depletion alone. This result suggests that H_2O_2 induces cofilin dephosphorylation through the action of SSH-1L in HeLa cells. The activation (phosphorylation) of LIMK1 was also observed with vanadate treatment or upon knockdown of SSH-1L in cells stimulated with H_2O_2 (Figure 1C). This result is consistent with the role of SSH-1L as a known phosphatase for LIMK1 (Soosairajah *et al.*, 2005).

14-3-3 Is a Key Regulator of SSH-1L-Cofilin Activation by H_2O_2

To establish that cellular SSH-1L activity was increased by H_2O_2, GST-SSH-1L was transiently transfected into HeLa cells for 16 h, and the cells were then treated with or without 0.5 M H_2O_2 for 30 min. GST-SSH-1L was isolated and then mixed with purified p-cofilin substrate in phosphatase buffer for 5–30 min to determine SSH-1L activity. We observed that SSH-1L activity was increased by H_2O_2 pretreatment compared with the control (Figure 2A). During these experiments, we assessed the interaction of SSH-1L with its endogenous negative regulator, 14-3-3 protein (Soosairajah *et al.*, 2005), as well as with the positive regulator, F-actin. We noticed that the interaction of GST-SSH-1L and 14-3-3ζ was decreased by H_2O_2, whereas binding to actin was increased (Figure 2A).

SSH proteins have been shown to be negatively regulated by phosphorylation of serine residues (Nagata-Ohashi *et al.*, 2004; Soosairajah *et al.*, 2005). Several 14-3-3 isoforms bind to sequences adjacent to these phosphorylated serine residues and act to suppress SSH-1L phosphatase activity (Nagata-Ohashi *et al.*, 2004; Soosairajah *et al.*, 2005). To test whether H_2O_2 might interfere with the 14-3-3/SSH-1L complex to promote SSH-1L activity, HeLa cells were transiently transfected with Myc-SSH-1L and were then either not stimulated or stimulated with H_2O_2. Again in the H_2O_2-treated cells, the binding of 14-3-3 proteins with SSH-1L was decreased compared with the control (Figure 2B). Together, these results suggest that the increase in SSH-1L activity induced by H_2O_2 may result from disruption of the inhibitory complex of SSH-1L and 14-3-3.

It is well known that ROS oxidatively modify a variety of signaling proteins, including protein kinases, phosphatases, and transcription factors (Cross and Templeton, 2006). The oxidation of 14-3-3ζ and 14-3-3γ has been previously described (Santpere *et al.*, 2007). We hypothesized that complexation of SSH-1L and 14-3-3 might be regulated by the H_2O_2-induced oxidation of one (or both) of the protein components. To test this hypothesis, we examined the oxidation status of SSH-1L and 14-3-3ζ proteins in the presence of H_2O_2 by labeling the proteins with 5-iodoacetamidofluorescein, which reacts with protein cysteine groups at pH 5.5 (Wu *et al.*, 1998). Although we could not detect significant

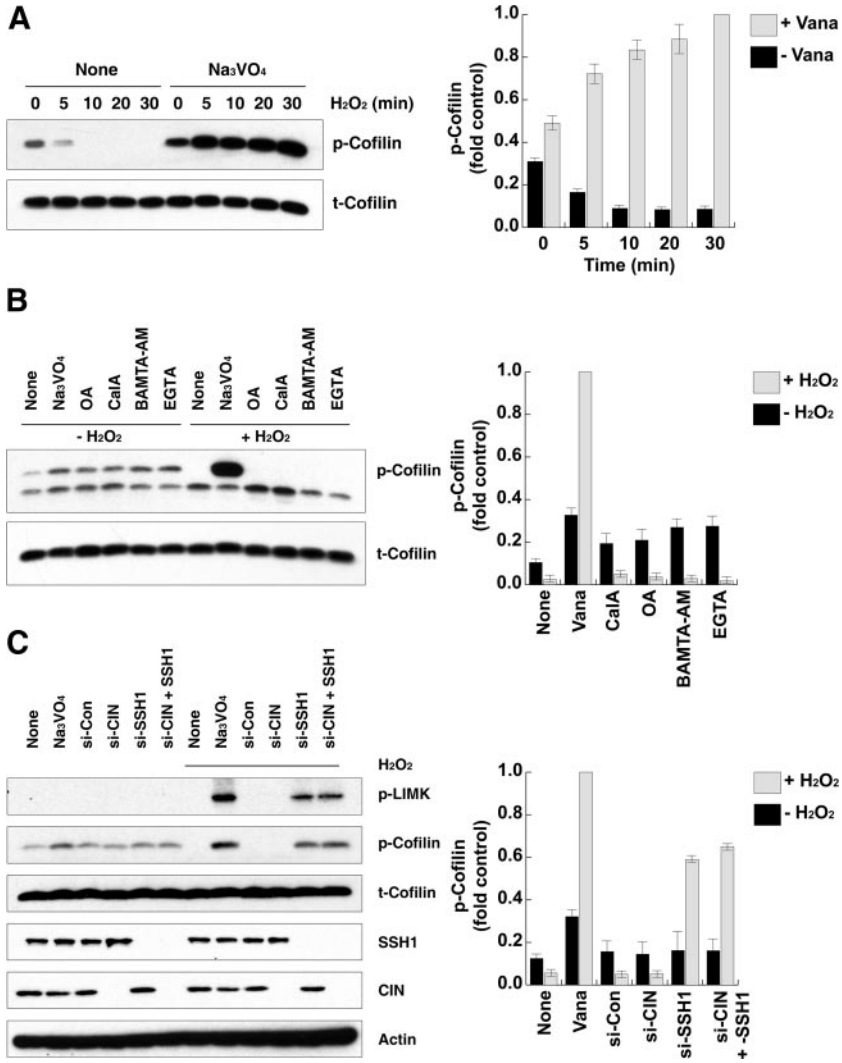

Figure 1. SSH-1L participates in H_2O_2-induced cofilin dephosphorylation. (A) HeLa cells were pretreated with or without 0.1 mM Na_3VO_4 for 30 min and then stimulated with 0.5 mM H_2O_2 for the indicated times. Cell lysates were immunoblotted with antibodies to phosphorylated cofilin (p-Cofilin) or cofilin (t-Cofilin). (B) HeLa cells were pretreated with or without the indicated inhibitor sets (1 mM Na_3VO_4, 1 μM okadaic acid [OA], 1 μM CalyculinA [CalA], 30 μM BAMTA-AM, 1 mM EGTA) for 0.5 h and then stimulated with 0.5 mM H_2O_2 for 30 min. Cell lysates were immunoblotted with antibodies to phosphorylated cofilin (p-Cofilin) or cofilin (t-Cofilin). (C) HeLa cells were transfected with 10 nM control, CIN or SSH-1L siRNA (si) for 48 h and then stimulated with or without 0.5 mM H_2O_2 for 30 min. Cell lysates were immunoblotted with antibodies to phosphorylated LIMK1/2 (p-LIMK), phosphorylated cofilin (p-Cofilin), cofilin (t-Cofilin), SSH-1L, CIN, or actin. (A–C) The graphs at the right of each panel represent the averaged normalized p-cofilin values; the value in Na_3VO_4 + H_2O_2-treated cells is taken as 1.0. Values are from three independent experiments ± SD.

oxidation of SSH-1L (nor of cofilin itself), we observed that 14-3-3ζ was significantly oxidized by H_2O_2 treatment (Figure 2C). These results support the hypothesis that 14-3-3 oxidation disrupts its inhibitory interaction with SSH-1L, leading to SSH-1L activation through its release from this complex.

H_2O_2 Induces Cofilin-Actin Rod Formation by Disrupting the SSH-1L-14-3-3 Interaction in Cofilin-GFP–expressing HeLa Cells

Cofilin and actin can be induced to aggregate to form rod-shaped cellular inclusions under specific chemical or physical conditions. Neurodegenerative stimuli, including energy stress and oxidative stress, act in neurons to induce cofilin/actin rod formation that disrupts distal neurite function. It has been established that such rod formation requires cofilin Ser3 dephosphorylation (Minamide *et al.*, 2000). We have recently shown that cellular energy depletion induced cofilin/actin rod formation in both a HeLa cell model system and in primary neurons and that this is dependent on an endogenous Hsp90-CIN biosensor (Huang *et al.*, 2008). Because H_2O_2 treatment induced substantial dephosphorylation of cofilin (Figure 1), we expected that H_2O_2 treatment might induce cofilin-actin rod formation in HeLa cells stably overexpressing eGFP cofilin. Indeed, we observed that H_2O_2 treatment dramatically induced cofilin/actin rod formation in cofilin-GFP–expressing HeLa cells (Figure 3, A and B). This H_2O_2-induced cofilin/actin rod formation was blocked by pretreatment with vanadate and was inhibited by knockdown of SSH-1L, but not CIN (Figure 3 and data not shown). Using this system as a readily quantifiable measure of SSH-1L cofilin phosphatase activity, we examined the effects of 14-3-3 protein on rod formation induced by H_2O_2. At early times of exposure to H_2O_2 (10 min), we found that expression of 14-3-3ζ-wt significantly reduced rod formation, whereas the nonbinding 14-3-3ζ-K49E mutant protein somewhat increased rod formation (Figure 3, A and B). Although the effects of SSH-1L knockdown were also observed after 30-min exposure to H_2O_2, the inhibitory effect of 14-3-3ζ-wt was substantially reduced. This is likely due to the oxidation of the majority of the 14-3-3ζ-wt protein after prolonged exposure to H_2O_2. These results support our biochemical data that H_2O_2 activates cofilin through a mechanism involving the dissociation of SSH-1L from 14-3-3ζ.

AngII-induced ROS Generation Activates Cofilin

AngII, acting via the AT1R, is a potent stimulus for ROS generation by Nox1 in smooth muscle and other cells

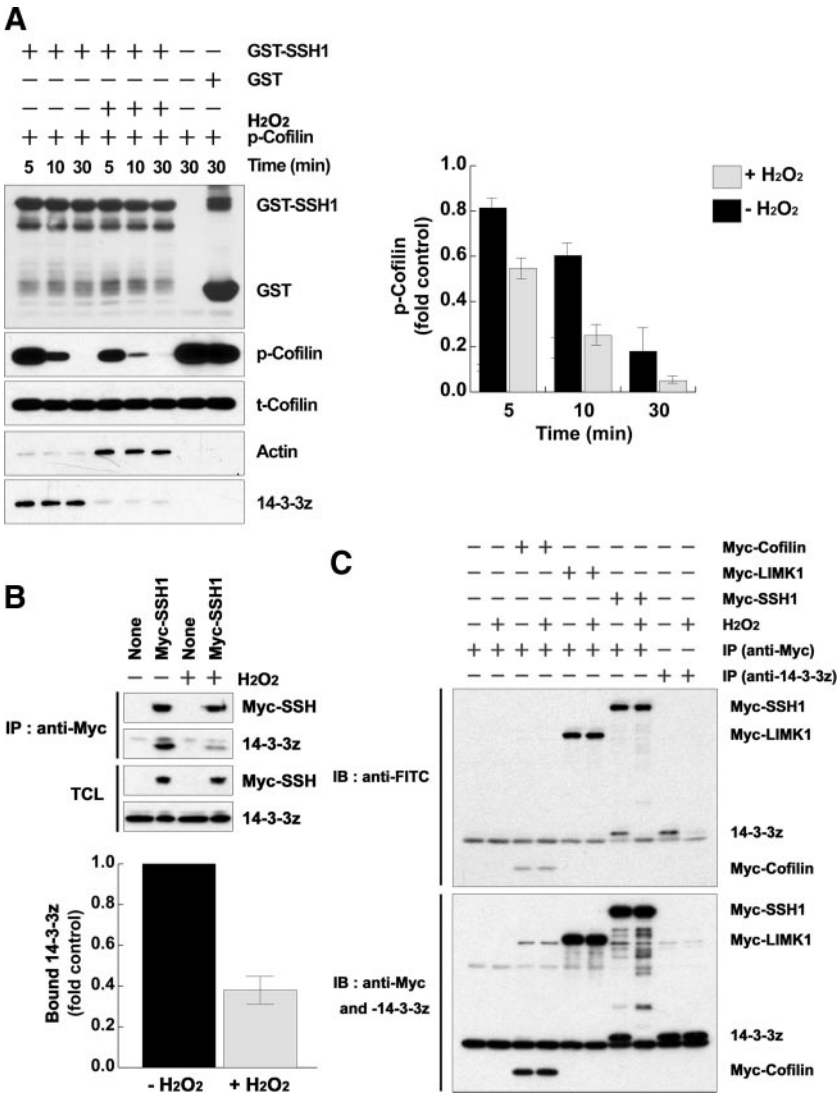

Figure 2. H_2O_2 disrupts the complex of SSH-1L and 14-3-3 through 14-3-3 oxidation. (A) HeLa cells were transfected with GST-SSH-1L for 18 h and then treated with H_2O_2 for 30 min. GST-SSH-1L proteins were precipitated from cell lysates and incubated with purified phosphocofilin for 0–30 min. Cofilin dephosphorylation was measured by immunoblotting with a phosphorylated cofilin antibody (p-Cofilin) and total cofilin, GST-SSH-1L, bound actin, or 14-3-3ζ were detected by immunoblotting with anti-cofilin, -GST, -actin, or -14-3-3ζ antibodies. The graph represents the averaged normalized p-cofilin values; the value with GST alone is taken as 1.0. Data are from three independent experiments ± SD. (B) HeLa cells transfected with empty vector (control) or myc-SSH-1L construct were treated with or without H_2O_2 for 30 min. The cells were then subject to lysis and immunoprecipitation with anti-myc antibodies. Immunoprecipitated Myc-SSH1L and bound 14-3-3 proteins were detected by immunoblotting with each anti-Myc or -pan-14-3-3 antibodies. The graph below represents averaged normalized bound 14-3-3 values; the value in Myc-SSH-1L–expressing cells treated without H_2O_2 is taken as 1.0. Data are from three independent experiments ± SD. (C) HeLa cells were transfected with the indicated cDNA for 18 h and then treated with or without H_2O_2 for 30 min. The cell lysates were prepared and proteins were labeled with 5′-iodoacetamidofluorescein (Wu *et al*., 1998). The labeled proteins were immunoprecipitated (IP) with anti-Myc or -14-3-3ζ antibodies, followed by immunoblotting (IB) with anti-FITC antibodies. The total immnoprecipitated proteins were analyzed by immunoblotting with anti-Myc or -14-3-3ζ antibodies. Oxidation of the redox-sensitive cysteine group(s) results in the loss of fluorescein labeling and thus the loss of anti-FITC reactivity. Representative experiments from three separate experiments are shown.

(Garrido and Griendling, 2008), and we confirmed this in the cofilin-GFP–expressing HeLa cells (Supplemental Figure S1, A and B). We examined whether such receptor-mediated Nox1 activation would stimulate endogenous cofilin activation/dephosphorylation. HeLa cells were cotransfected with AT1R along with Nox1 and its required cofactors, NoxA1 and NoxO1 (referred to collectively as Nox1s), then stimulated with 100 ng/ml AngII. As shown in Figure 4A, the level of p-cofilin was decreased after 5–10 min of agonist addition, followed by an increase to slightly greater than basal levels at 30 min. In the presence of the flavoenzyme Nox inhibitor DPI, AngII stimulation of cofilin dephosphorylation was blocked, indicating the requirement for ROS formation in this process (Figure 4B). Similarly wortmannin, an inhibitor of the downstream mediator of AngII signaling to Nox1, PI 3-kinase (Choi *et al.*, 2008), also blocked cofilin dephosphorylation (Figure 4B). Consistent with our earlier results using H_2O_2, the overexpression of 14-3-3ζ-wt inhibited cofilin activation compared with control cells, whereas the nonbinding 14-3-3ζ-K49E mutant had no inhibitory effect in AngII-stimulated HeLa cells (Figure 4C).

We observed that AngII stimulation induced the disruption of the SSH-1L-14-3-3ζ complex (Figure 4D), and this effect was again blocked by PI 3-kinase inhibitor and DPI, indicating it resulted from AngII signaling–induced ROS formation. The AngII-stimulated disruption of the SSH-1L-14-3-3ζ complex was associated with increased oxidation of 14-3-3ζ stimulated by AngII in a time-dependent manner (Figure 4E), and this effect was also inhibited by DPI and wortmannin treatment (Figure 4F). These results strongly suggest that ROS formation induced by the AngII-stimulated activation of Nox1 activates the SSH-1L-cofilin pathway through 14-3-3 oxidation.

Nox1 localizes with cofilin to areas of AngII-induced cytoskeletal remodeling

We next examined whether AngII would induce cofilin rod formation in cofilin-GFP–expressing HeLa cells that also express the AT1R and Nox1s. Similar to the time course of AngII-induced cofilin activation (Figure 4A), we observed cofilin rod formation at 5–10 min after AngII stimulation, which disappeared by 30 min after stimulation (Figure 5A). In contrast, cofilin-GFP–expressing HeLa cells coexpressing only the AT1R (and lacking endogenous Nox) did not form rods at any time after AngII addition (Figure 5A). Interestingly, the morphology of the AT1R-expressing HeLa cells was changed by AngII stim-

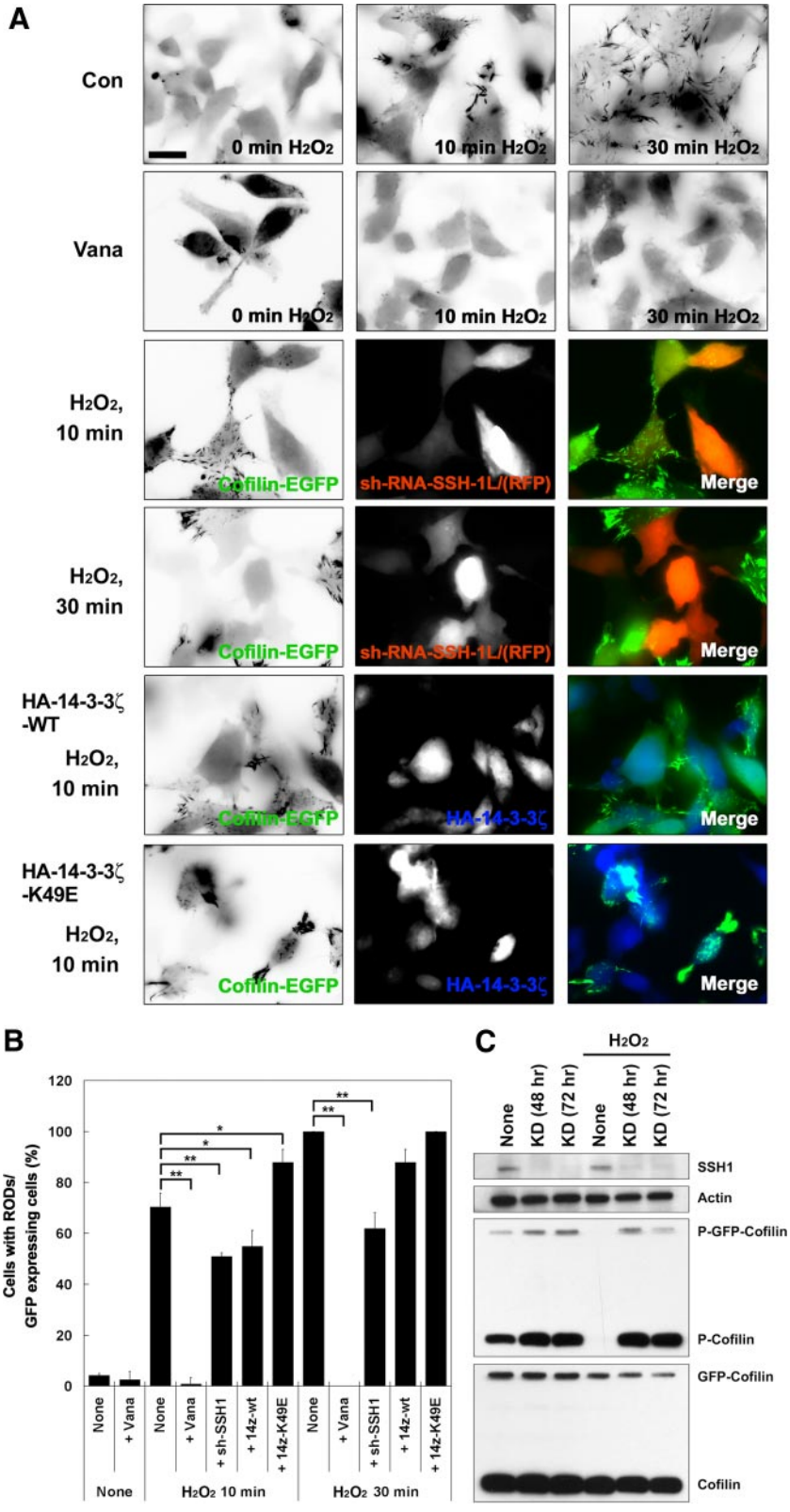

Figure 3. H_2O_2 induces cofilin rod formation in cofilin-GFP–expressing HeLa cells. (A) Cofilin-GFP–expressing HeLa cells transfected with or without sh-RNA-SSH-1L/RFP, 14-3-3ζ-wt, or 14-3-3ζ-K49E were treated with or without H_2O_2 for up to 30 min, as indicated. The eGFP-cofilin images are presented as inverted fluorescence images to highlight rod formation. The merged images show eGFP-Cofilin (green), sh-RNA-SSH-1L/RFP (red), or HA-14-3-3ζ (blue). Scale bar, 10 μm. (B) Cofilin rod formation is quantified and represented graphically. The percentage of rod-forming cofilin-GFP–expressing HeLa cells was scored as the total number of rod-containing cells/total GFP-positive cells. The number of rods observed in H_2O_2-treated cells at 30 min was set to 100%. The average ± SD of three experiments is shown, where a minimum of 100 cells were scored for each time point (* $p > 0.05$; ** $p > 0.01$). (C) Protein expression level of the cells treated with sh-RFP-SSH-1L was confirmed using Western blotting with anti-SSH-1L, -actin, -phosphorylated cofilin, or -cofilin antibodies. Knockdown (KD) of SSH-1L prevented the H_2O_2-induced loss of p-Cofilin and p-GFP-Cofilin. Representative experiments from three separate experiments are shown.

ulation, with the cells assuming a polarized phenotype where eGFP-cofilin localized to peripheral membranes (Figure 5B). Cells expressing Nox1s alone (i.e., no receptor) showed no response to AngII stimulation. However, in the presence of both AT1R and Nox1s, the cells became highly ruffled in response to AngII (Figure 5B, graph), and we observed that eGFP-cofilin colocalized with Myc-Nox1s or F-actin within peripheral membrane ruffles following AngII stimulation (Figure 5B, see enlarged insets).

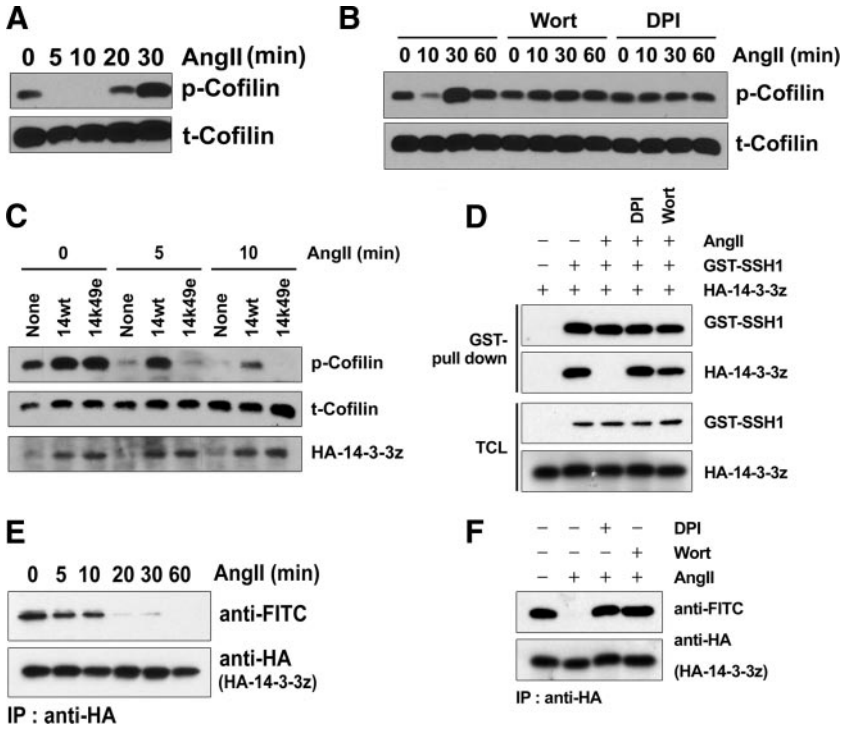

Figure 4. AngII dephosphorylates cofilin through the ROS-dependent dissociation of SSH-1L from 14-3-3. (A–F) HeLa cells were cotransfected with AT1R and Nox1s (Nox1, NoxO1, and NoxA1) for 18 h and then serum-starved for 16 h. (A) The cells were stimulated with 0.1 μg/ml AngII for the indicated times. Cell lysates were immunoblotted with antibodies to phosphorylated cofilin (p-Cofilin) or cofilin (t-Cofilin). (B) The cells were pretreated with or without 100 nM wortmannin (Wort) or 10 μM DPI for 30 min and then stimulated with 0.1 μg/ml AngII for the indicated times. Cell lysates were immunoblotted with antibodies to phosphorylated cofilin (p-Cofilin) or cofilin (t-Cofilin). (C) The cells cotransfected with or without HA-14-3-3ζ-wt or HA-K49E mutant were stimulated with 0.1 μg/ml AngII for the indicated times. Cell lysates were immunoblotted with antibodies to phosphorylated cofilin (p-Cofilin), cofilin (t-Cofilin), or HA (HA-14-3-3ζ). (D) The cells cotransfected with or without GST-SSH-1L or HA-14-3-3ζ-wt were pretreated with or without 10 μM DPI or 100 nM wortmannin (Wort) for 30 min and then stimulated with 0.1 μg/ml AngII for the indicated times. GST pulldown of proteins from cell lysates and the total cell lysates (TCL) were immunoblotted with antibodies to GST (GST-SSH-1L) or HA (HA-14-3-3ζ). (E) Cells were stimulated with 0.1 μg/ml AngII for the indicated times. Cell lysates were prepared and proteins labeled with 5′-iodoacetamide fluorescein, as in *Materials and Methods.* HA-14-3-3ζ was immunoprecipitated with anti-HA antibodies, followed by immunoblotting with anti-FITC antibodies. The total immunoprecipitated HA-14-3-3ζ was analyzed by immunoblotting with anti-HA antibodies. Loss of anti-FITC reactivity is indicative of protein oxidation. (F) The cells were pretreated with or without 10 μM DPI or 100 nM wortmannin (Wort) for 30 min and then stimulated with 0.1 μg/ml AngII for 30 min. Cell lysates were prepared and proteins were labeled with 5′-iodoacetamide fluorescein. The HA-14-3-3ζ was immunoprecipitated with anti-HA antibodies, followed by immunoblotting with anti-FITC antibodies. The total immunoprecipitated HA-14-3-3ζ was analyzed by immunoblotting with anti-HA antibodies. (A–F) Representative experiments from three separate experiments are shown.

AngII and ROS-dependent Motility Requires SSH-1L, Is Modulated by 14-3-3ζ, and Is Associated with Redox Regulation of 14-3-3ζ

ROS formation and SSH-1L activity are required for AngII-induced wound closure (Figure 6A). Wound healing of AngII-stimulated HeLa cells is suppressed by both wortmannin and DPI treatment, as well as by the expression of 14-3-3ζ-wt, but not the inactive K49E mutant. A similar mechanism appears to be operative in MCF-7 breast cancer cells that express endogenous AT1R and the Nox2 system. Here ROS production induced by AngII is also associated with increased cell motility, as assessed in both a wound healing assay (Figure 6B) and in a filter-based assay (Figure 6C). Again, the AngII-induced motility was reduced when SSH-1L was depleted using siRNA and was decreased by expression of 14-3-3ζ-wt. Stimulation of MCF-7 motility by AngII was accompanied by the decrease in phosphocofilin levels, and this was correlated with the oxidation of endogenous 14-3-3ζ (Figure 6D). These data suggest the control of AngII-induced cofilin activation through the redox-dependent regulation of the cofilin phosphatase, SSH-1 is an important component of AngII-stimulated motility.

DISCUSSION

Here we identify a novel mechanism through which ROS directly modulates the dynamics of the actin cytoskeleton. The redox-induced oxidation of 14-3-3ζ in inhibitory complexes with SSH-1L decreases its binding to SSH-1L, thereby releasing the active phosphatase to dephosphorylate and activate cofilin. Whether this represents preferential oxidation of 14-3-3 in the complex with SSH-1L or whether there is oxidation of the larger cellular 14-3-3 pool is unclear. Because 14-3-3 proteins are known to bind to and regulate a variety of phosphorylated structural and signaling proteins, it would be of interest to determine whether the redox-mediated oxidation of 14-3-3 may influence other signaling processes as well. The presence of oxidized forms of 14-3-3ζ and 14-3-3γ in Alzheimer's disease has been described (Santpere *et al.*, 2007). However, the protein oxidation observed under these circumstances appears to involve glycooxidative damage that results in the irreversible loss of 14-3-3 protein function. Reversible oxidation (e.g., of cysteine residues) would be more likely to be involved in cellular signal transduction.

In the studies described here, we used both exogenous H_2O_2 directly as a source of ROS, as well as ROS generated endogenously through the action of AT1R-regulated Nox1 activity. In each case, ROS formation induced the dephosphorylation of cellular cofilin (Figures 1A and 4A). The loss of Ser3-phosphocofilin was dependent on the activity of the cofilin phosphatase SSH-1L, but not on CIN or other phosphatases with activity toward cofilin (Figure 1C). SSH-1L has also been shown to be a phosphatase for activated LIMK1 (Soosairajah *et al.*, 2005). Consistent with this, we found that the cellular levels of Ser505 phospho-LIMK1 increased substantially when SSH-1L, but not CIN, was depleted using siRNA (Figure 1C). Because LIMK1 phosphorylation at Ser505 in the activation loop is indicative of

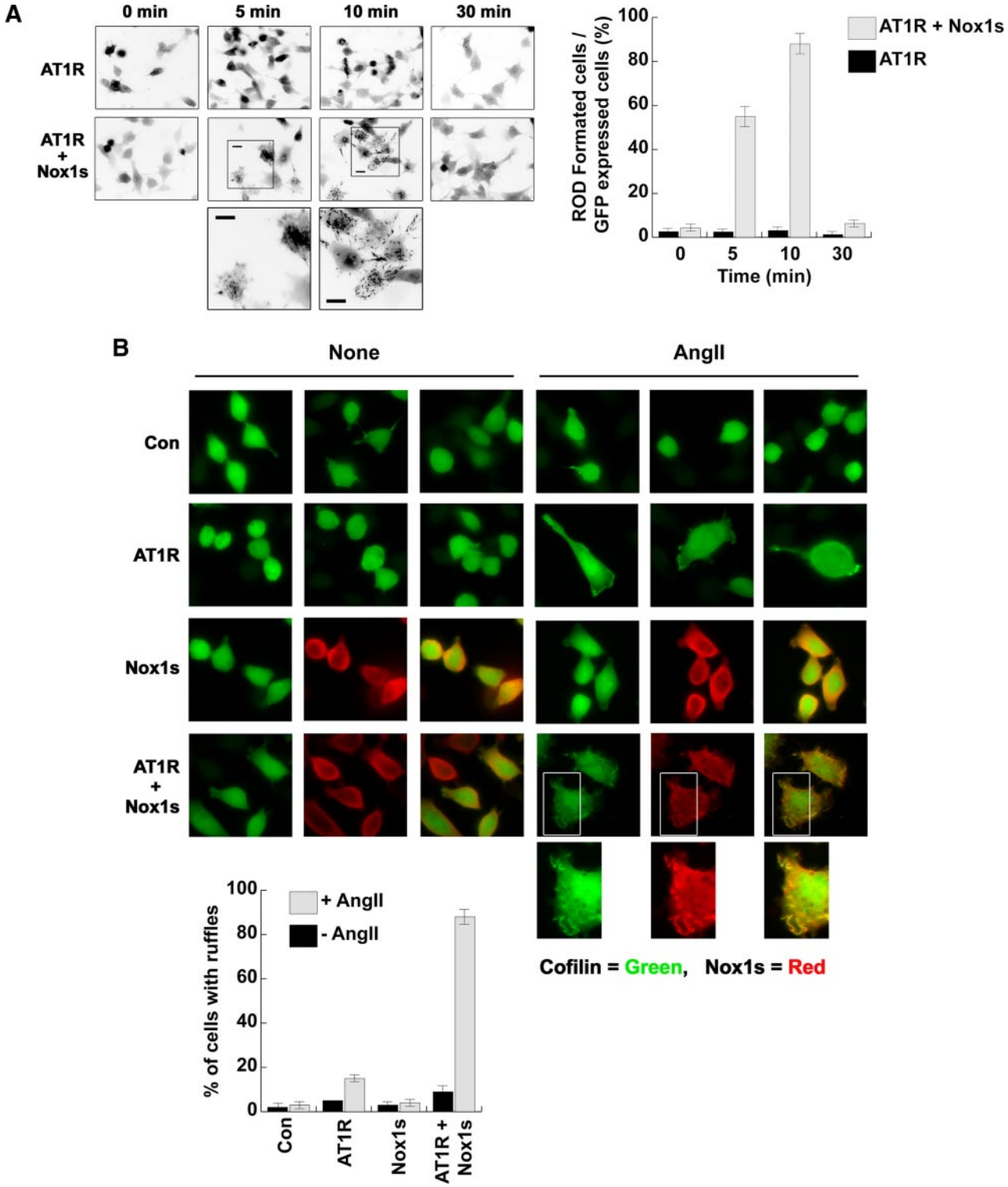

Figure 5. AngII induces cofilin rod formation in cofilin-GFP–expressing HeLa cells. (A) Cofilin-GFP–expressing HeLa cells cotransfected with AT1R and/or Nox1s were stimulated with 0.1 μg/ml AngII for the indicated times. The eGFP-cofilin images are presented as inverted fluorescence images to highlight rod formation. Magnified images of eGFP-cofilin rods within the boxed areas are presented at the bottom; scale bar, 10 μm. Cofilin rod formation was quantified and data are shown graphically. The percentage of rod-forming cofilin-GFP–expressing HeLa cells was scored as the total number of rod-containing cells/total GFP-positive cells. The average ± SD of three experiments is shown, where a minimum of 100 cells were scored for each time point. (B) Cofilin-GFP–expressing HeLa cells cotransfected with AT1R, Nox1s, or both the AT1R and Nox1s (as indicated) were either unstimulated (None) or were stimulated with 0.1 μg/ml AngII for 30 min. The cells were fixed for immunostaining against Myc-Nox1s (red) and/or eGFP-cofilin (green). Overlap in the merged images (rightmost panels of the Nox1s and AT1R + Nox1s samples) shows up as yellow. Magnified images of the boxed areas under this condition are presented at bottom; scale bar, 10 μm. The percentage of cells developing ruffles after ±AngII stimulation is shown for cells transfected with indicated cDNA sets. The average ± SD of three experiments is shown, where a minimum of 50 cells was scored.

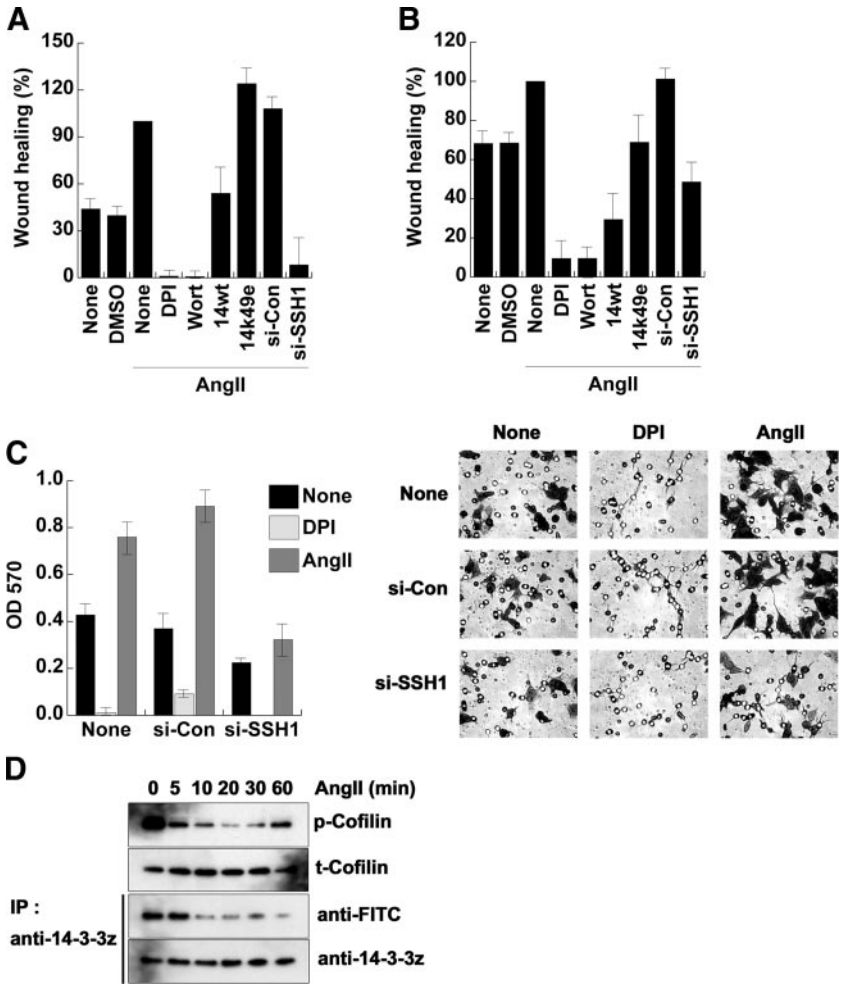

Figure 6. AngII-induced cell migration is dependent on ROS and SSH-1L. (A and B) Confluent HeLa (A) or MCF-7 (B) cells seeded onto 60-mm culture dishes were wounded, washed twice with PBS, and treated with or without DMSO or 0.1 μg/ml AngII, as described in *Materials and Methods.* Phase-contrast images were taken 24 h after wounding and treatment, and the number of cells migrating into the wounded area was determined using ImageJ software. Cells were pretreated with DPI (10 μM) or Wort (100 nM) as indicated for 30 min before AngII stimulation. Another set of cells was transfected with 14-3-3ζ-wt, -K49E, siRNA-con, or siRNA-SSH-1L for 48 h before seeding onto dishes. 100% of wound healing is defined for AngII-stimulated cells. (C) MCF-7 cells were transfected with or without siRNA (si)-control or siRNA-SSH-1L RNA for 48 h and then transwell migration assays were performed as described in *Materials and Methods.* (A–C) Averages ± SD or n = 3 experiments. (D) MCF-7 cells were stimulated with 0.1 μg/ml AngII for the indicated times. Cell lysates were immunoblotted with antibodies to phosphorylated cofilin (p-Cofilin) or cofilin (t-Cofilin) and labeled with 5′-iodoacetamide fluorescein, as in *Materials and Methods.* The labeled proteins were immunoprecipitated (IP) with anti-14-3-3ζ antibodies, followed by immunoblotting with anti-FITC antibodies. The total immnoprecipitated proteins were analyzed by immunoblotting with anti-14-3-3ζ antibody. Loss of anti-FITC reactivity is indicative of protein oxidation. A representative experiment from two separate experiments is shown.

enzyme activation, these data suggest that the loss of SSH-1L activity both reduces cofilin Ser3 dephosphorylation and increases its phosphorylation via LIMK1. We observed no activation of LIMK1 upon treatment with H_2O_2 alone (Figure 1C).

14-3-3 is known to be a negative regulator of SSH-1L activity. Soosairajah *et al.* (2005) showed that 14-3-3ζ binds to phosphorylated SSH-1L, but not to the more active nonphosphorylated SSH-1L, and the presence of 14-3-3ζ reduces the binding of SSH-1L to F-actin. Kligys *et al.* (2007) proposed that an unknown, Rac GTPase-regulated phosphatase may disrupt the interaction of SSH-1L and 14-3-3ζ to release catalytically active SSH-1L. We established that there was a pre-existing complex of SSH-1L and 14-3-3ζ in unstimulated HeLa cells and that H_2O_2 treatment induced the dissociation of SSH-1L from 14-3-3ζ (Figure 2). This led to an increase in SSH-1L phosphatase activity and increased binding of SSH-1L to its positive regulator, F-actin (Figure 2A). Of particular note, the decrease in the ability of 14-3-3ζ to bind to SSH-1L was associated with the formation of a highly oxidized state of 14-3-3ζ by H_2O_2 (Figure 2C). In contrast, no significant oxidation of SSH-1L, LIMK1, or cofilin was detected. Therefore, our data suggest that the oxidation of 14-3-3ζ is required to disrupt complex formation and activate SSH-1L during H_2O_2-induced activation.

Recently, a cofilin phosphatase-dependent mechanism for the formation of cofilin-actin rods in response to energy stress has been described (Huang *et al.*, 2008). As part of these studies, a model system for rod formation by ATP depletion was developed by preparing a stable HeLa cell line expressing slightly higher than endogenous levels of eGFP-cofilin. In these cofilin-GFP–expressing HeLa cells, cofilin rod formation is directly correlated with dephosphorylation of both endogenous cofilin and eGFP-cofilin (Huang *et al.*, 2008). We used this system to confirm our in vitro biochemical results (Figure 3). Thus, we showed that cofilin-actin rod formation was induced by treatment with H_2O_2, and that this was significantly reduced by the knockdown of SSH-1L. We note however that there was only a partial reduction of rod formation even when SSH-1L protein was depleted by more than 80%; this likely indicates that additional mechanisms to decrease the levels of cellular P-cofilin are operative in these cells, including via the endogenous Hsp90-CIN sensor we previously described (Huang *et al.*, 2008). The expression of 14-3-3ζ-wt, but not the nonphosphosubstrate-binding 14-3-3ζ-K49E mutant, significantly reduced rod formation induced by H_2O_2 as well (Figure 3, A and B). These results support the operation of a redox-sensitive mechanism to regulate cofilin dephosphorylation involving both SSH-1L and 14-3-3ζ.

To examine the effects of ROS generated internally via an NADPH oxidase, we used the well-characterized AT1R-Nox1 system. We showed that AngII-induced, DPI-sensitive, and Nox1-mediated ROS production also caused cofilin activation, SSH-1L activation, and dissociation from 14-3-3ζ (Figure 4). This was again associated with the oxidation of

14-3-3ζ (Figure 4, E and F). However, although there was no reversal of 14-3-3ζ oxidation over the 60-min time course, we observed that cofilin phosphorylation was restored at later times (Figure 4A). This could be due to the inactivation of another, late-acting cofilin phosphatase (i.e., chronophin) or the inactivation of SSH itself by 14-3-3–independent mechanisms. Alternatively, this may result from increased LIMK activity at later times after stimulation, as reported in other studies (Nishita *et al.*, 2005; San Martin *et al.*, 2008). Of note, the dephosphorylation of cofilin induced by AngII in the presence of Nox1s was associated with both transient cofilin/actin rod formation in cofilin-eGFP-HeLa cells, as well as with more prolonged substantial membrane ruffling (Figure 5). Under these conditions, components of the Nox1 system were observed to colocalize with cofilin in the membrane ruffles (Figure 5B).

The reorganization of the actin cytoskeleton at the leading edge of eukaryotic cells is a fundamental aspect of cell motility, and requires the coordinated function of both actin-polymerizing and actin-depolymerizing/severing factors. To drive the cell anterior forward, branched actin filaments are generated at the leading edge through the action of the Arp2/3 complex and/or filamin A. Actin-depolymerizing components, including proteins of the cofilin/ADF (actin-depolymerizing factor) family, disassemble F-actin within the actin network to recycle actin monomers to the leading edge for further rounds of polymerization (Bamburg, 1999). We suggest that the mechanism described contributes to the action of ROS in modulating cofilin-mediated actin dynamics during cell migration.

It has been shown that cell motility induced by AngII (Ushio-Fukai *et al.*, 2001) and other growth factors (Schroder *et al.*, 2007) requires Nox1-derived ROS. The mechanisms contributing to regulation of the actin cytoskeletal machinery during ROS-regulated motility have not been elucidated. However, changes in the phosphorylation state of the actin-severing/-depolymerizing factor, cofilin, have been noted (San Martin *et al.*, 2008; Lee *et al.*, 2009). We demonstrate here a mechanism by which ROS directly regulates the dephosphorylation and activation of cofilin—through the redox-mediated oxidation of 14-3-3ζ to disrupt an inhibitory complex with the cofilin phosphatase SSH-1L. We have observed that both ROS formation and SSH-1L activity are required for AngII-induced wound closure (Figure 6A). A similar mechanism appears to be operative in MCF-7 breast cancer cells that express endogenous AT1R and the Nox2 system. Here ROS production induced by AngII is also associated with increased cell motility, as assessed in both a wound healing assay (Figure 6B) and in a filter-based assay (Figure 6C). Consistently, the AngII-induced motility required SSH-1L- and was decreased by expression of 14-3-3ζ. Our data indicate the control of cofilin activation through the redox-dependent regulation of the cofilin phosphatase, SSH-1 during AngII-receptor–induced cell motility.

At least in AngII-stimulated HeLa cells expressing Nox1, the Nox enzyme appears to localize to regions of the cell undergoing active actin rearrangements (e.g., ruffling). This may enable the localized action of ROS generated by Nox1 on cofilin activity and thus the spatial and temporal modulation of actin dynamics required for motility. The mechanisms regulating localized formation of ROS and their contributions to leading edge actin dynamics should be of interest to investigate.

ACKNOWLEDGMENTS

The authors thank members of the Bokoch laboratory for comments and criticisms. This work was supported by National Institutes of Health Grants HL48008 and GM44428 to G.M.B. T.Y.H. is supported by a postdoctoral fellowship from the American Heart Association, Western affiliate.

REFERENCES

Ambach, A., Saunus, J., Konstandin, M., Wesselborg, S., Meuer, S. C., and Samstag, Y. (2000). The serine phosphatases PP1 and PP2A associate with and activate the actin-binding protein cofilin in human T lymphocytes. Eur. J. Immunol. *30*, 3422–3431.

Arber, S., Barbayannis, F. A., Hanser, H., Schneider, C., Stanyon, C. A., Bernard, O., and Caroni, P. (1998). Regulation of actin dynamics through phosphorylation of cofilin by LIM-kinase. Nature *393*, 805–809.

Bamburg, J. R. (1999). Proteins of the ADF/cofilin family: essential regulators of actin dynamics. Annu. Rev. Cell Dev. Biol. *15*, 185–230.

Bedard, K., and Krause, K. H. (2007). The NOX family of ROS-generating NADPH oxidases: physiology and pathophysiology. Physiol. Rev. *87*, 245–313.

Bokoch, G.M., and Knaus, U.G. (2003). NADPH oxidases: not just for leukocytes anymore! Trends Biochem. Sci. *28*, 502–508.

Choi, H., Leto, T. L., Hunyady, L., Catt, K. J., Bae, Y. S., and Rhee, S. G. (2008). Mechanism of angiotensin II-induced superoxide production in cells reconstituted with angiotensin type 1 receptor and the components of NADPH oxidase. J. Biol. Chem. *283*, 255–267.

Cohen, P. (1990). The structure and regulation of protein phosphatases. Adv. Second Messenger Phosphoprot. Res. *24*, 230–235.

Condeelis, J. (1993). Life at the leading edge: the formation of cell protrusions. Annu. Rev. Cell Biol. *9*, 411–444.

Cross, J. V., and Templeton, D. J. (2006). Regulation of signal transduction through protein cysteine oxidation. Antioxid. Redox Signal. *8*, 1819–1827.

Deshayes, F., and Nahmias, C. (2005). Angiotensin receptors: a new role in cancer? Trends Endocrinol. Metab. *16*, 293–299.

Djordjevic, T., Pogrebniak, A., BelAiba, R. S., Bonello, S., Wotzlaw, C., Acker, H., Hess, J., and Gorlach, A. (2005). The expression of the NADPH oxidase subunit p22phox is regulated by a redox-sensitive pathway in endothelial cells. Free Radic. Biol. Med. *38*, 616–630.

Garrido, A. M., and Griendling, K. K. (2008). NADPH oxidases and angiotensin II receptor signaling. Mol. Cell. Endocrinol. *302*, 148–158.

Gohla, A., Birkenfeld, J., and Bokoch, G. M. (2005). Chronophin, a novel HAD-type serine protein phosphatase, regulates cofilin-dependent actin dynamics. Nat. Cell Biol. *7*, 21–29.

Heyworth, P. G., Robinson, J. M., Ding, J., Ellis, B. A., and Badwey, J. A. (1997). Cofilin undergoes rapid dephosphorylation in stimulated neutrophils and translocates to ruffled membranes enriched in products of the NADPH oxidase complex. Evidence for a novel cycle of phosphorylation and dephosphorylation. Histochem. Cell Biol. *108*, 221–233.

Higgs, H. N., and Pollard, T. D. (2001). Regulation of actin filament network formation through ARP2/3 complex: activation by a diverse array of proteins. Annu. Rev. Biochem. *70*, 649–676.

Huang, T. Y., DerMardirossian, C., and Bokoch, G. M. (2006). Cofilin phosphatases and regulation of actin dynamics. Curr. Opin. Cell Biol. *18*, 26–31.

Huang, T. Y., Minamide, L. S., Bamburg, J. R., and Bokoch, G. M. (2008). Chronophin mediates an ATP-sensing mechanism for cofilin dephosphorylation and neuronal cofilin-actin rod formation. Dev. Cell *15*, 691–703.

Ikeda, S., Yamaoka-Tojo, M., Hilenski, L., Patrushev, N. A., Anwar, G. M., Quinn, M. T., and Ushio-Fukai, M. (2005). IQGAP1 regulates reactive oxygen species-dependent endothelial cell migration through interacting with Nox2. Arterioscler. Thromb. Vasc. Biol. *25*, 2295–2300.

Ishikawa, K., Takenaga, K., Akimoto, M., Koshikawa, N., Yamaguchi, A., Imanishi, H., Nakada, K., Honma, Y., and Hayashi, J. (2008). ROS-generating mitochondrial DNA mutations can regulate tumor cell metastasis. Science *320*, 661–664.

Kim, J. S., Diebold, B. A., Babior, B. M., Knaus, U. G., and Bokoch, G. M. (2007). Regulation of Nox1 activity via protein kinase A-mediated phosphorylation of NoxA1 and 14-3-3 binding. J. Biol. Chem. *282*, 34787–34800.

Kim, J. S., *et al.* (2006). Transforming growth factor-beta1 regulates macrophage migration via RhoA. Blood *108*, 1821–1829.

Kligys, K., *et al.* (2007). The slingshot family of phosphatases mediates Rac1 regulation of cofilin phosphorylation, laminin-332 organization, and motility behavior of keratinocytes. J. Biol. Chem. *282*, 32520–32528.

Lambeth, J. D., Kawahara, T., and Diebold, B. (2007). Regulation of Nox and Duox enzymatic activity and expression. Free Radic. Biol. Med. *43*, 319–331.

Lassegue, B., and Clempus, R. E. (2003). Vascular NAD(P)H oxidases: specific features, expression, and regulation. Am. J. Physiol. Regul. Integr. Comp. Physiol. *285*, R277–R297.

Lassegue, B., Sorescu, D., Szocs, K., Yin, Q., Akers, M., Zhang, Y., Grant, S. L., Lambeth, J. D., and Griendling, K. K. (2001). Novel gp91(phox) homologues in vascular smooth muscle cells: nox1 mediates angiotensin II-induced superoxide formation and redox-sensitive signaling pathways. Circ. Res. *88*, 888–894.

Laurent, E., McCoy, J. W., 3rd, Macina, R. A., Liu, W., Cheng, G., Robine, S., Papkoff, J., and Lambeth, J. D. (2008). Nox1 is over-expressed in human colon cancers and correlates with activating mutations in K-Ras. Int. J. Cancer *123*, 100–107.

Lee, C. K., *et al.* (2006). Proteomic profiling and identification of cofilin responding to oxidative stress in vascular smooth muscle. Proteomics *6*, 6455–6475.

Lee, M. Y., *et al.* (2009). Mechanisms of vascular smooth muscle NADPH oxidase 1 (Nox1) contribution to injury-induced neointimal formation. Arterioscler. Thromb Vasc. Biol. *29*, 480–487.

Mehta, P. K., and Griendling, K. K. (2007). Angiotensin II cell signaling: physiological and pathological effects in the cardiovascular system. Am. J. Physiol. Cell Physiol. *292*, C82–C97.

Minamide, L. S., Striegl, A. M., Boyle, J. A., Meberg, P. J., and Bamburg, J. R. (2000). Neurodegenerative stimuli induce persistent ADF/cofilin-actin rods that disrupt distal neurite function. Nat. Cell Biol. *2*, 628–636.

Moldovan, L., Moldovan, N. I., Sohn, R. H., Parikh, S. A., and Goldschmidt-Clermont, P. J. (2000). Redox changes of cultured endothelial cells and actin dynamics. Circ. Res. *86*, 549–557.

Munnamalai, V., and Suter, D. M. (2009). Reactive oxygen species regulate F-actin dynamics in neuronal growth cones and neurite outgrowth. J. Neurochem. *108*, 644–661.

Nagata-Ohashi, K., *et al.* (2004). A pathway of neuregulin-induced activation of cofilin-phosphatase Slingshot and cofilin in lamellipodia. J. Cell Biol. *165*, 465–471.

Nishita, M., Tomizawa, C., Yamamoto, M., Horita, Y., Ohashi, K., and Mizuno, K. (2005). Spatial and temporal regulation of cofilin activity by LIM kinase and Slingshot is critical for directional cell migration. J. Cell Biol. *171*, 349–359.

Niwa, R., Nagata-Ohashi, K., Takeichi, M., Mizuno, K., and Uemura, T. (2002). Control of actin reorganization by Slingshot, a family of phosphatases that dephosphorylate ADF/cofilin. Cell *108*, 233–246.

Nonaka, Y., Iwagaki, H., Kimura, T., Fuchimoto, S., and Orita, K. (1993). Effect of reactive oxygen intermediates on the in vitro invasive capacity of tumor cells and liver metastasis in mice. Int. J. Cancer *54*, 983–986.

Pruyne, D., Evangelista, M., Yang, C., Bi, E., Zigmond, S., Bretscher, A., and Boone, C. (2002). Role of formins in actin assembly: nucleation and barbed-end association. Science *297*, 612–615.

Ridley, A. J., Schwartz, M. A., Burridge, K., Firtel, R. A., Ginsberg, M. H., Borisy, G., Parsons, J. T., and Horwitz, A. R. (2003). Cell migration: integrating signals from front to back. Science *302*, 1704–1709.

Sadok, A., Bourgarel-Rey, V., Gattacceca, F., Penel, C., Lehmann, M., and Kovacic, H. (2008). Nox1-dependent superoxide production controls colon adenocarcinoma cell migration. Biochim. Biophys. Acta *1783*, 23–33.

San Martin, A., Lee, M. Y., Williams, H. C., Mizuno, K., Lassegue, B., and Griendling, K. K. (2008). Dual regulation of cofilin activity by LIM kinase and Slingshot-1L phosphatase controls platelet-derived growth factor-induced migration of human aortic smooth muscle cells. Circ. Res. *102*, 432–438.

Santpere, G., Puig, B., and Ferrer, I. (2007). Oxidative damage of 14-3-3 zeta and gamma isoforms in Alzheimer's disease and cerebral amyloid angiopathy. Neuroscience *146*, 1640–1651.

Schroder, K., Helmcke, I., Palfi, K., Krause, K. H., Busse, R., and Brandes, R. P. (2007). Nox1 mediates basic fibroblast growth factor-induced migration of vascular smooth muscle cells. Arterioscler. Thromb. Vasc. Biol. *27*, 1736–1743.

Soares, F. A., Shaughnessy, S. G., MacLarkey, W. R., and Orr, F. W. (1994). Quantification and morphologic demonstration of reactive oxygen species produced by Walker 256 tumor cells in vitro and during metastasis in vivo. Lab. Invest. *71*, 480–489.

Soosairajah, J., Maiti, S., Wiggan, O., Sarmiere, P., Moussi, N., Sarcevic, B., Sampath, R., Bamburg, J. R., and Bernard, O. (2005). Interplay between components of a novel LIM kinase-slingshot phosphatase complex regulates cofilin. EMBO J. *24*, 473–486.

Svitkina, T. M., and Borisy, G. G. (1999). Arp2/3 complex and actin depolymerizing factor/cofilin in dendritic organization and treadmilling of actin filament array in lamellipodia. J. Cell Biol. *145*, 1009–1026.

Szatrowski, T. P., and Nathan, C. F. (1991). Production of large amounts of hydrogen peroxide by human tumor cells. Cancer Res. *51*, 794–798.

Tonks, N. K. (2005). Redox redux: revisiting PTPs and the control of cell signaling. Cell *121*, 667–670.

Ushio-Fukai, M. (2009). Compartmentalization of redox signaling through NADPH oxidase-derived ROS. Antioxid. Redox Signal. (*in press*).

Ushio-Fukai, M., Griendling, K. K., Becker, P. L., Hilenski, L., Halleran, S., and Alexander, R. W. (2001). Epidermal growth factor receptor transactivation by angiotensin II requires reactive oxygen species in vascular smooth muscle cells. Arterioscler. Thromb. Vasc. Biol. *21*, 489–495.

Wang, W., Eddy, R., and Condeelis, J. (2007). The cofilin pathway in breast cancer invasion and metastasis. Nat. Rev. Cancer *7*, 429–440.

Wang, Y., Shibasaki, F., and Mizuno, K. (2005). Calcium signal-induced cofilin dephosphorylation is mediated by Slingshot via calcineurin. J. Biol. Chem. *280*, 12683–12689.

Weber, D. S., Taniyama, Y., Rocic, P., Seshiah, P. N., Dechert, M. A., Gerthoffer, W. T., and Griendling, K. K. (2004). Phosphoinositide-dependent kinase 1 and p21-activated protein kinase mediate reactive oxygen species-dependent regulation of platelet-derived growth factor-induced smooth muscle cell migration. Circ. Res. *94*, 1219–1226.

Wu, R. F., Gu, Y., Xu, Y. C., Nwariaku, F. E., and Terada, L. S. (2003). Vascular endothelial growth factor causes translocation of p47phox to membrane ruffles through WAVE1. J. Biol. Chem. *278*, 36830–36840.

Wu, W. S. (2006). The signaling mechanism of ROS in tumor progression. Cancer Metastasis Rev. *25*, 695–705.

Wu, Y., Kwon, K. S., and Rhee, S. G. (1998). Probing cellular protein targets of H2O2 with fluorescein-conjugated iodoacetamide and antibodies to fluorescein. FEBS Lett. *440*, 111–115.

Yamaguchi, H., and Condeelis, J. (2007). Regulation of the actin cytoskeleton in cancer cell migration and invasion. Biochim. Biophys. Acta *1773*, 642–652.

Yang, N., Higuchi, O., Ohashi, K., Nagata, K., Wada, A., Kangawa, K., Nishida, E., and Mizuno, K. (1998). Cofilin phosphorylation by LIM-kinase 1 and its role in Rac-mediated actin reorganization. Nature *393*, 809–812.